ROTORCRAFT FUSELAGE DRAG ESTIMATION METHOD FOR CONCEPTUAL DESIGN PHASE

Fatih YILMAZ, fatih.yilmaz4@tai.com.tr, Turkish Aerospace Industries Inc. (Türkiye)
Abdullah Enes COSKUN, abdullahenes.coskun@tai.com.tr, Turkish Aerospace Industries Inc. (Türkiye)
Hasan IBACOGLU, hasan.ibacoglu@tai.com.tr, Turkish Aerospace Industries Inc. (Türkiye)
Muammer KILCIK, muammer.kilcik@tai.com.tr, Turkish Aerospace Industries Inc. (Türkiye)
Tolga KAYABASI, tolga.kayabasi@tai.com.tr, Turkish Aerospace Industries Inc. (Türkiye)

Abstract

This study examines various fuselage parameters that was predicted to have a significant effect on rotorcraft fuselage drag in a design space generated by statistical engineering tools. The paper begins with a discussion about boundaries and aims of the conceptual design phase. It then explains the level of detail of the work and the reasons for working at this level of detail. Finally, the aerodynamic and statistical analysis of the design space is presented. At the end of the study, the reader is presented with graphs which were obtained from an empirical equation to show how each parameter changes the helicopter fuselage and what changes can be made.

1. NOTATION

Symbols

β	Upsweep angle, deg

Acronyms:

ANN	Artificial Neural Networks
CAD	Computer-Aided Design
CCD	Central Composite Design
CCP	Cabin Conic Parameter
CFD	Computational Fluid Dynamics
CLn	Nondimensionalized Cabin Length
CWn	Nondimensionalized Cabin Width
DoE	Design of Experiments
FFD	Full Factorial Design
FPDA	Flat Plate Drag Area
GCR	Glass Corner Radius
GCRn	Nondimensionalized GCR
GENN	Gradient Enhanced Neural Networks
HPC	High-Performance Computing
NLn	Nondimensionalized Nose Length
QP	Quadratic Programming
RSM	Response Surface Methodology
SMT	Surrogate Modelling Toolbox

2. INTRODUCTION

The conceptual design phase creates roadmaps for all aspects of the project/design, including key decisions, research, and evaluation. To explore new ideas, discover applicable technologies, and analyse capabilities that may mature into the launch of a new project; many companies that design unique products for their users use an exploratory research activity in the conceptual design phase (Ref. 1). Exploratory research with the right steps provides organizations with a wide range of forecasts from the beginning of the project (Ref. 2). These forecasts provide some of the parameters that are crucial from day one in the design and manufacture of the rotorcraft, such as an accurate estimate of the committed cost (Ref. 3), preliminary weight, specific fuel consumption and early estimates of drag characteristics.

The main purpose of accurately estimating the rotorcraft performance characteristics, such as drag, is to know the power to be expended and therefore the amount of fuel to be expended to obtain that power. The importance of reducing the power required by the rotorcraft is becoming increasingly apparent with the new generation of high-speed rotorcraft and the energy consumption required by new rotorcraft designs. Stepniewski (Ref. 4), discussed that the per capita energy consumption of current rotorcraft configurations is generally higher than that of other short-distance transport options. According to Keys & Wiesner (Ref. 5), the greatest reduction in power is achieved by reducing parasite drag, which accounts for more than 40% of the total power required.

To carry out an exploratory study on a rotorcraft, it is very important to be able to set the fidelity correctly. To estimate the drag value of the rotorcraft correctly, the parameters to be studied must satisfy all the necessary and sufficient conditions, but each additional parameter increases the computational cost significantly. Therefore, there must be a certain number of cases that should be sufficient to understand the drag characteristics and should not overburden the computational capabilities in terms of cost. In more rigorous studies, the number of parameters or the number of values taken in the parameters may increase to get further accuracy. In this paper, the estimation calculations were conducted following Full Factorial Design (FFD) as it is commonly used in Response Surface Methodology (RSM) (Ref. 6).

The study aims to provide the fuselage drag output of the rotorcraft with an acceptable accuracy at the requirements identification stages. The iterative steps to achieve this output are explained in the following sections, respectively. Section 3 describes which parameters are determined in design space generation and the value ranges of these parameters. Section 4 focuses on the Computational Fluid Dynamics (CFD) perspective, where the analyses are performed under which conditions and with which turbulence models. Section 5 focuses on the statistical point of view, first defining and explaining the model in which the design space is created, and then explaining the analysis results obtained. Section 6 is the results section. Concluding remarks on the study and future studies are discussed in Section 7.

3. DESIGN SPACE GENERATION

Keys & Wiesner discussed the component-based drag breakdown. The main rotor hub, landing gear, and basic fuselage geometry are responsible for more than 60% of the drag produced. This paper focuses only on basic fuselage drag levels and how to reduce them. Certain fuselage properties were selected to observe the change in drag characteristics.

3.1. Selected Fuselage Properties

Even very small changes that can be made to the rotorcraft will affect its drag characteristics. Recognizing this, studies were carried out to find the fuselage properties that affect the drag characteristics. A standard rotorcraft was analysed in three sections.

3.1.1. Cabin Section

Three parameters have been chosen for this section. These are Cabin Conic Parameter (CCP) (Figure 1), cabin width (Figure 2), and cabin length (Figure 3) CCP is a parameter that is inherently defined in the CATIA V5 (Ref. 7) software's wireframe tools. It defines the curvature of the curve that connects the top of the cabin to the side reference line of the cabin from the front view of the fuselage.

Figure 1: CCP comparison between extrema values

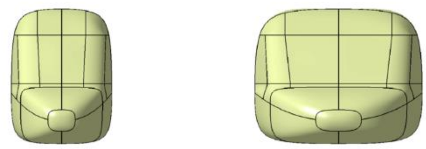

Figure 2: Cabin width comparison between extrema values

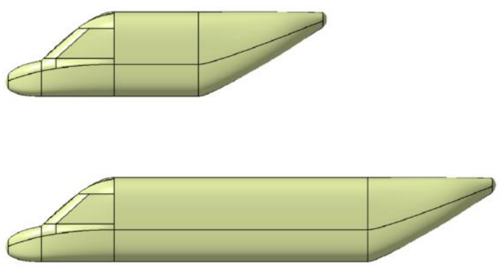

Figure 3: Cabin length comparison between extrema values

3.1.2. Nose & Cockpit Section

Considering the fact that the design of the nose and cockpit section is mostly shaped concerning certain factors such as pilot ergonomics and placements of communication systems; the aerodynamic design of that section might be overlooked. The reason is mostly the fact that these factors are given higher priority than aerodynamics due to their critical impact on the functionality, safety, and operational requirements of the rotorcraft. However, carrying out the sensitivity analyses (see Section 5) and reviewing the recommendations of Keys & Wiesner, it was decided to have two parameters in this fuselage section. These parameters are the cabin corner radius (Figure 4) and the nose length (Figure 5)**.** Nose length to nose height ratio is kept at 1 in all cases.

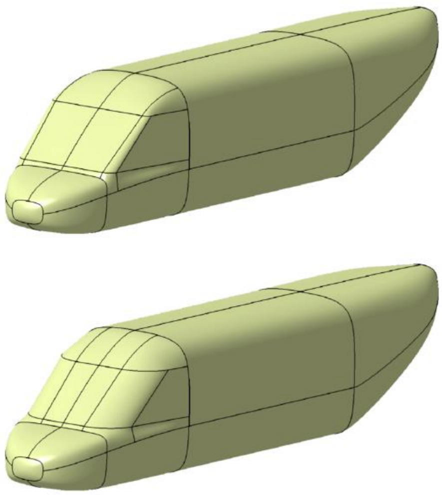

Figure 4: GCR comparison between extrema values

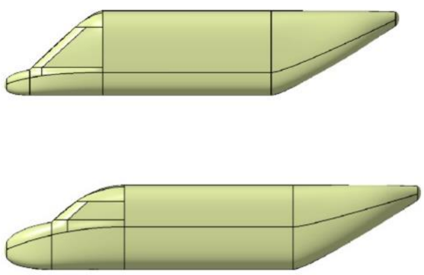

Figure 5: Nose length comparison between extrema values

3.1.3. Aft Section

The aft section of a rotorcraft plays a critical role in stability, control, and overall aerodynamic performance. The design of the aft section involves a trade-off between several factors, including drag reduction, stability, control effectiveness, and structural integrity. Depending on the mission profile of the helicopter to be designed, the inclusion or exclusion of a ramp plays an important role in the design of the aft section. One parameter of the aft section is included in the study. This parameter has been defined as the angle between the bottom line of the cabin and the tail boom inclination line from the side view of the fuselage. It is called the upsweep angle (β) (Figure 6). In the forthcoming plans of this study, when the tail and tail rotor are included in the model, it is expected that more parameters from the aft section will have a role in the determination of the drag characteristics.

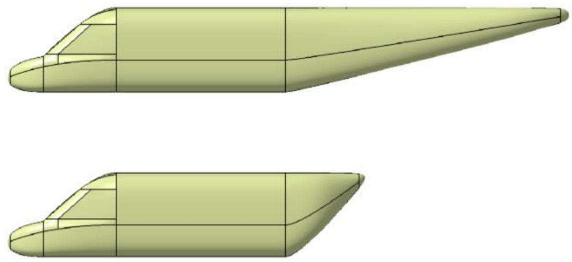

Figure 6: β comparison between extrema values

3.2. Component Value Determination

While evaluating parametric variables, it was found appropriate to use dimensionless variables for the current design problem. Non-dimensional variables reduce the number of variables used to describe a system and therefore reduce the requirements for recreating that system. Therefore, a parameter from the geometric model was chosen for the non-dimensionalization of the parameters described above. This non-dimensionalization parameter is identical in all models. In this paper, this parameter was determined as the height of the fuselage and was set at 1800 mm (=5.9 ft).

For this study, it was planned to choose 3 values for each of the 6 parameters. To determine the values of the parameters, present rotorcrafts in similar class were looked through. After determining the upper and lower limits, another value was chosen in the middle of these two extrema. The selected parameters and their values are shown in Table 1. The values in the table represent the non-dimensionalized values with the predetermined reference value.

Table 1: Selected parameters and examined values

Parameters	Min Value	Median Value	Max Value
Cabin Width	0.75	1.0	1.25
Upsweep Angle	15	32.5	50
CCP	0.6	0.7	0.8
Cabin length	1.0	2.0	3.0
Nose length	0.3	0.42	0.56
GCR	0.05	0.15	0.25

3.3. Parametric Fuselage Model

To study the aerodynamic performance of a basic fuselage, a parametric Computer-Aided Design (CAD) model was created in CATIA V5. The design of a new fuselage from the sketch, rather than using an existing fuselage, allows all selected parameters to be changed independently on the rotorcraft fuselage. Therefore, the change in aerodynamic performance can be studied both separately and simultaneously as a function of the geometric parameters.

4. AERODYNAMIC ANALYSIS METHODS

In this section, the determination of aerodynamic tools, turbulence models, and their near-wall applications are explained.

4.1. Determination of Aerodynamic Tool

Aerodynamic analysis tools have different levels of fidelity, i.e. the degree of accuracy and detail in the simulation of airflow around objects. In conventional studies, high levels of fidelity in computation may not be required at the conceptual design phase. However, the cost of computing for this study only, was a less important variable due to the capacity of the high-performance computing (HPC) systems. In this context, it was decided to use CFD methods because of the desire to understand the characteristics more accurately. Star-CCM+ (Ref. 8) was preferred as both the mesh generation software and the solver.

4.2. Determination of Turbulence Model

After agreeing on CFD, studies were started on which turbulence model to work on. The search for a helicopter fuselage to compare and a paper analysing this fuselage was started, both to validate the systems and to investigate the accuracy of the turbulence models. The validation started with the verification of the aerodynamic model on the ROBIN fuselage provided by NASA for academic purposes (Ref. 9). Acikgoz's study was selected for comparison (Ref. 10) since it shares drag coefficient values for different solution methods. Since the fidelity required for aerodynamic analyses at the conceptual design stage is relatively low compared to later design stages, the feasibility of performing the analyses at one of the lowest fidelities was investigated. In this context, the Spalart-Allmaras (S-A) (Ref. 13) turbulence model was tested for validation on the 3.15 m (10,335 ft) ROBIN fuselage. The comparison results are shown in Table 2. As can be seen in Table 2, it was observed that the absolute error values mostly decreased up to a point and started to fluctuate around 2-3.5%. For this reason, it was decided that approximately 2 million meshes would be sufficient for the studies.

4.3. Near-Wall Applications

The boundary layer performance of a turbulence model refers to its ability to accurately capture the behaviour of the turbulent boundary layer near the wall, which is effective for phenomena such as separation, reattachment, and transition. This calculation is performed with a dimensionless coefficient called y+ and the value of y+ can be chosen more flexibly for the Spalart-Allmaras turbulence model than for the k-epsilon and k-omega models. In this context, y+ = 30 was chosen for the analyses and the first layer length of the boundary layer was derived from this value.

Table 2: Comparison of solutions for accuracy

Mesh count (millions)	Acikgoz (Ref. 10)	S-A Solution	Absolute % Error
0.4	0.006978	0.006147	11.915399
0.5	0.006978	0.006121	12.279654
0.7	0.006978	0.006114	12.382811
0.9	0.006978	0.006181	11.420074
1.0	0.006978	0.006361	8.844974
1.2	0.006978	0.006543	6.234594
1.7	0.006978	0.006789	2.709151
2.6	0.006978	0.006962	0.232638
3.0	0.006978	0.007092	1.638213
3.7	0.006978	0.007150	2.465743
4.8	0.006978	0.007208	3.300012
6.2	0.006978	0.007191	3.054778
8.1	0.006978	0.007167	2.702861
9.6	0.006978	0.007154	2.524058
13.0	0.006978	0.007145	2.393546

5. STATISTICAL APPROACH

Accurate estimation of helicopter fuselage drag is essential for optimizing rotorcraft design and performance. CFD analysis, combined with statistical methods, provides a powerful approach to predicting and understanding the aerodynamic characteristics of the fuselage. This section presents the application of RSM, for helicopter fuselage drag estimation based on CFD data. It also discusses the use of Design of Experiments (DoE) techniques, specifically Central Composite Design (CCD) and FFD, and the decision to move from CCD to FFD when the expected results were not obtained.

5.1. Response Surface Methodology

Response Surface Methodology (RSM) is a robust statistical approach employed to model and optimize intricate systems characterized by multiple variables. The primary objective of RSM is to establish a mathematical relationship between the input variables, also known as factors, and the response variable, which in the context of this study is helicopter fuselage drag. By employing a series of strategically designed experiments, RSM efficiently explores the multidimensional design space and constructs a response surface. This response surface is a fitted mathematical model that captures the underlying relationships between the input variables and the response (Ref. 12).

The application of RSM for helicopter fuselage drag estimation involves the careful selection of a set of experimental design points, each representing a distinct combination of design variables such as β, CCP, and non-dimensionalized versions of cabin length, nose length, glass corner radius (GCR) and cabin width. CFD simulations are then performed on these design points to obtain corresponding fuselage drag values, which serve as the response variable data required for the RSM analysis.

In this study, the JMP software (Ref. 13) was utilized to conduct a robust analysis by fitting the RSM model using the multiple regressions through the widely recognized Least Squares (LS) method. The primary objective of the RSM was to establish a comprehensive mathematical representation in the form of a second-degree polynomial that captures the complex relationship between fuselage geometry and helicopter fuselage drag. This regression model effectively captures the behaviour of the response surface and facilitates the estimation of fuselage drag at any unexplored combination of design variables within the investigated range.

5.2. Design of Experiments

Due to the substantial computational costs entailed in conducting CFD analysis, the optimization of simulation efficiency while preserving result accuracy emerged as a primary concern in this study. To effectively address this challenge, the Orthogonal Central Composite Design (OCCD) method readily available in JMP software was used. Orthogonal CCD, also known as the Box-Wilson design, was used to strategically minimize the number of simulations while ensuring the construction of a robust RSM (Ref. 14).

The Orthogonal CCD method adeptly explores the design space by furnishing 53 distinct combinations of the design factors, chosen to represent a comprehensive and well-balanced experimental design. This unique combination of factorial points, center points, and star points facilitated the achievement of an optimized and statistically sound data collection framework.

Upon thorough analysis of the acquired data and the subsequent development of the Response Surface

Model, we were met with an impressive R-squared value of 0.99. This remarkable coefficient signifies that the Response Surface Model adeptly captures the inherent variability in the response variable, which, in our investigation, constitutes the helicopter fuselage drag. However, when the results of the CCD were examined, it was observed that the changes in the parameters could not be fully captured. Comparison of CCD and FFD with actual CFD values are given in Figure 7, Figure 8, and Figure 9.

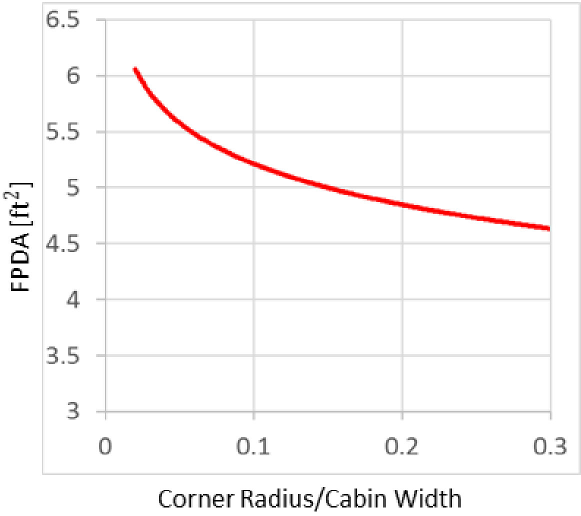

Figure 7: Change trends of drag force with change of one parameter, GCR.

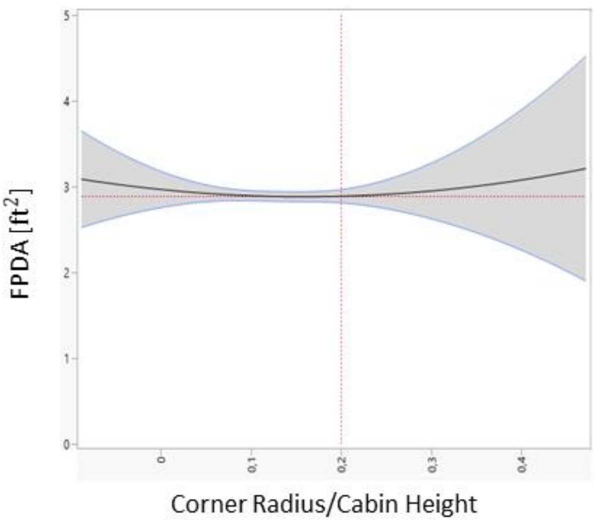

Figure 8: Change trends of drag force with change of one parameter, GCR, and its estimation with CCD.

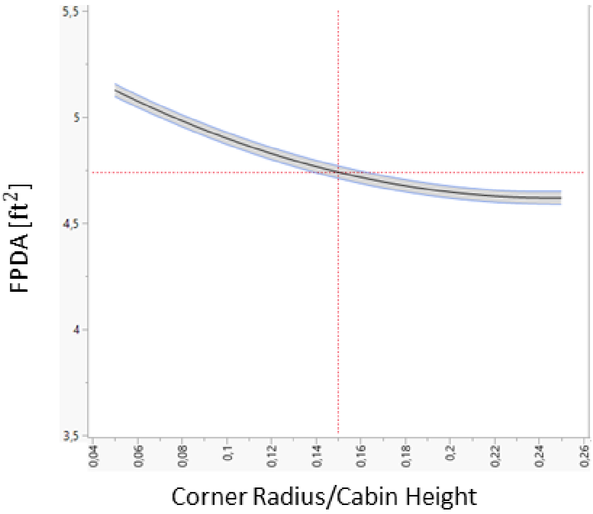

Figure 9: Change trends of drag force with change of one parameter, GCR, and its estimation with FFD.

In Figure 7, there is a monotonously decrease in the fashion of FPDA with respect to corner radius/cabin width. This result was obtained via CFD analyses. In Figure 8, the prediction profile of FPDA with respect to corner radius/cabin height using orthogonal CCD method can be seen. The grey zones indicate confidence intervals that are dependent on the factor. This dependency becomes relatively large that the monotonous fashion which was expected according to CFD results may be hindered. There are possibilities to gather invalid predictions, like an increasing or constant fashion. Consequently, CCD method was found to be insufficient. In Figure 9, the same prediction profile of Figure 8 using FFD method can be observed. It is apparent that the confidence intervals are more consistent than that of CCD results. Furthermore, it can also be observed that the expected fashion of FPDA can be obtained. It should be noted that selected points for analyses are slightly different between Figure 7 and that of Figure 8 and Figure 9. Moreover, the non-dimensionalization of corner radius in the horizontal axis of Figure 7 is defined with respect to cabin width, while that of Figure 8 and Figure 9 are defined with respect to cabin height. This difference only affects numerical values; they do not have an impact on the fashion that was the focus of this comparison. After detecting the insufficiency of CCD, FFD was applied.

Within the scope of FFD, 729 total geometric cases were prepared for 3 different values of 6 parameters. These geometric cases have been solved with

Spalart-Allmaras turbulence model. The next section presents the results of foretold applications.

6. RESULTS

6.1. Prediction Profiler Plots

Prediction profiler plots display the outputs (values on the Y-axis) for each input (values on the X-axis) and plot profile traces. A profile trace is the predicted response when one variable is changed while the other variables are held constant at their current values. Prediction profiler plots are one of the ways to observe the change in one variable at a time and observing the effect on the predicted response (Ref 15). Prediction profile plots for the 6 foretold parameters are given from Figure 10 to Figure 15.

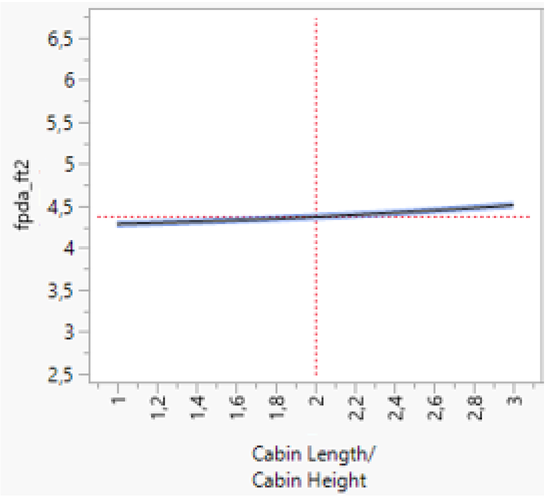

Figure 10: Prediction profile of non-dimensionalized cabin length parameter.

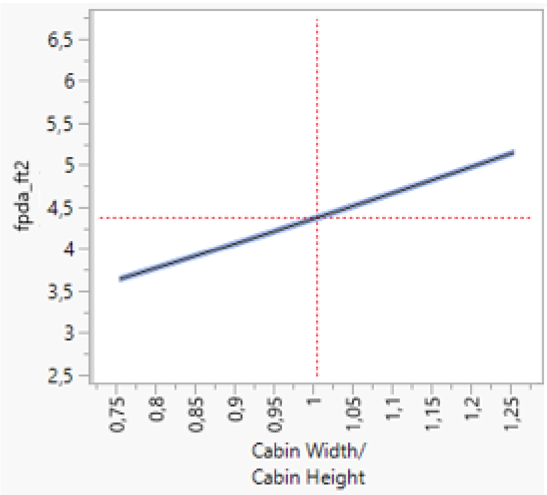

Figure 11: Prediction profile of non-dimensionalized cabin width parameter.

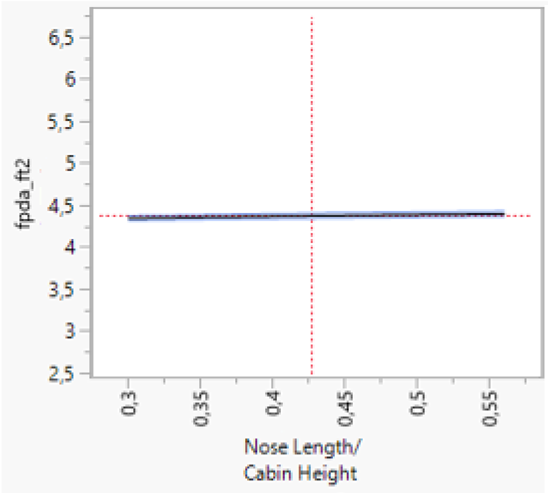

Figure 12: Prediction profile of non-dimensionalized nose length parameter.

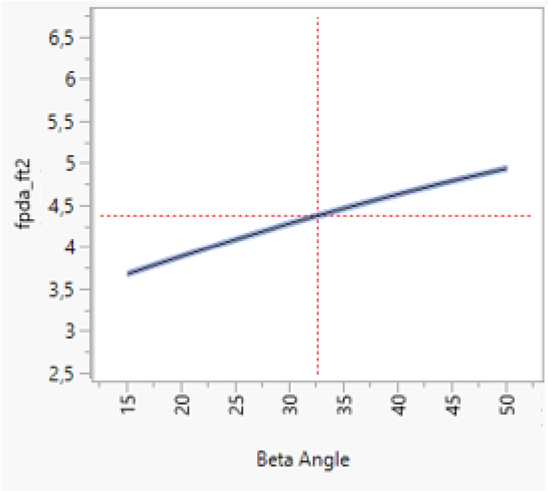

Figure 13: Prediction profile of β parameter.

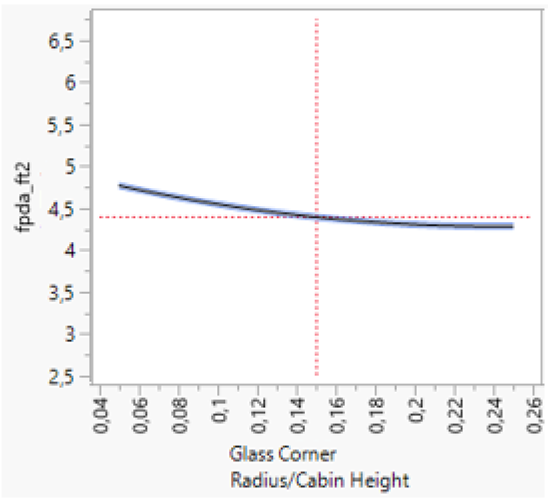

Figure 14: Prediction profile of non-dimensionalized GCR parameter.

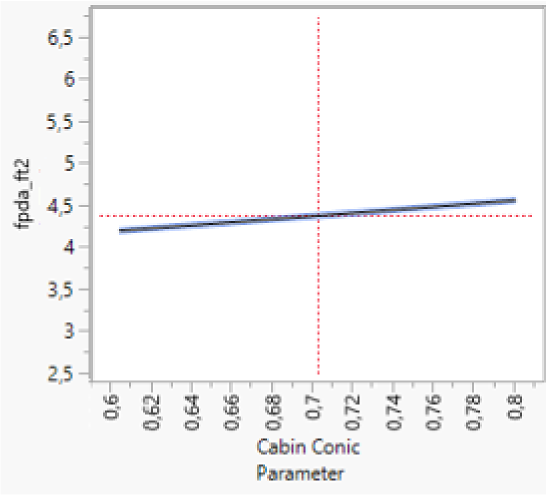

Figure 15: Prediction profile of CCP.

6.2. Actual by Predicted Plot

Drag changes due to β, CCP and non-dimensionialized versions of cabin length, nose length, GCR and cabin width are given. After conducting the CFD analyses (see Section 4) and statistical operations (see Section 5), one prediction formula was obtained in order to represent the combinational effect of the parameters on total Flat Plate Drag Area (FPDA) of the basic fuselage. Reference area for the FPDA calculation was chosen as the frontal area. In addition to the prediction formula, statistical accuracy and quality of the estimation are also obtained accordingly.

The comparison of the predicted versus actual values can be seen in Figure 16. Average absolute percent error between actual values and prediction of all cases is calculated as 1.93% (R^2: 0.98, $p < 0.01$).

6.3. Prediction Equation

The prediction equation used to obtain the plot given in Figure 16 is given in Equation (1). Since the equation operates within a range restricted by strict boundaries, the constants in the equation are formed by named constants ranging from 1 to 28. The values entered into the subtraction process with the dimensionless parameters represent the median values of the determined parameters.

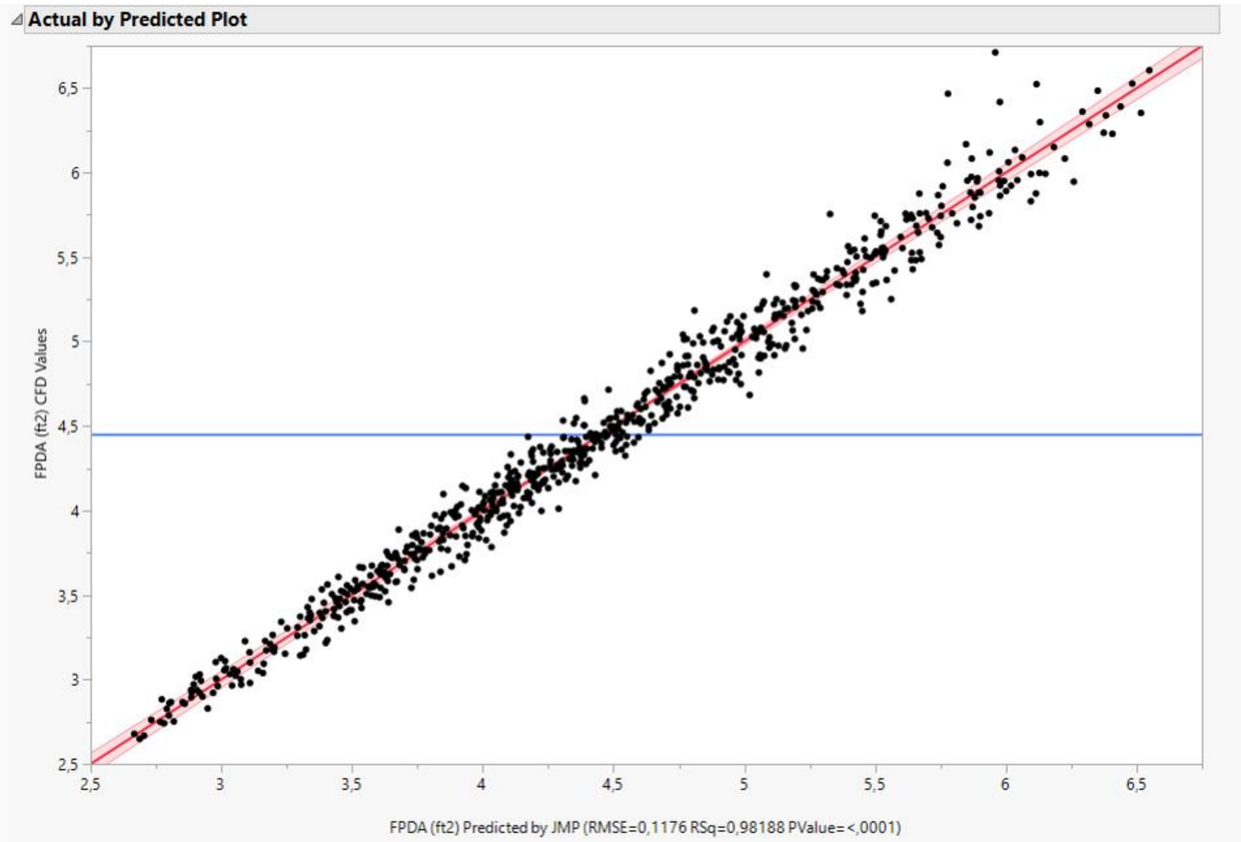

Figure 16: Actual by predicted plot of FPDA values.

$$
\begin{aligned}
\boldsymbol{FPDA} = {} & C_1 + C_2 \times CLn + C_3 \times CWn + C_4 \times NLn + C_5 \times \beta + C_6 \times GCRn + C_7 \times CCP \\
& + (CLn - 2) \times \big((CLn - 2) \times C_8\big) + (CLn - 2) \times \big((CWn - 1) \times C_9\big) \\
& + (CWn - 1) \times \big((CWn - 1) \times C_{10}\big) + (CLn - 2) \times \big((NLn - 0.42) \times C_{11}\big) \\
& + (CWn - 1) \times \big((NLn - 0.42) \times C_{12}\big) + (NLn - 0.42) \times \big((NLn - 0.42) \times C_{13}\big) \\
& + (CLn - 2) \times \big((\beta - 32.5) \times C_{14}\big) + (CWn - 1) \times \big((\beta - 32.5) \times C_{15}\big) \\
& + (NLn - 0.42) \times \big((\beta - 32.5) \times -C_{16}\big) + (\beta - 32.5) \times \big((\beta - 32.5) \times C_{17}\big) \\
& + (CLn - 2) \times \big((GCRn - 0.15) \times C_{18}\big) + (CWn - 1) \times \big((GCRn - 0.15) \times C_{19}\big) \\
& + (NLn - 0.42) \times \big((GCRn - 0.15) \times C_{20}\big) + (\beta - 32.5) \times \big((GCRn - 0.15) \times C_{21}\big) \\
& + (GCRn - 0.15) \times \big((GCRn - 0.15) \times C_{22}\big) + (CLn - 2) \times \big((CCP - 0.7) \times C_{23}\big) \\
& + (CWn - 1) \times \big((CCP - 0.7) \times C_{24}\big) + (NLn - 0.42) \times \big((CCP - 0.7) \times -C_{25}\big) \\
& + (\beta - 32.5) \times \big((CCP - 0.7) \times C_{26}\big) + (GCRn - 0.15) \times \big((CCP - 0.7) \times C_{27}\big) \\
& + (CCP - 0.7) \times \big((CCP - 0.7) \times C_{28}\big)
\end{aligned} \tag{1}
$$

7. CONCLUSION

This paper started with a discussion about the conceptual design phase in terms of fidelity of computational studies. Parameter determination of a basic fuselage and their value selection was told. The aerodynamic and statistical point of view to this subject was explained. Observing the prediction formula and its comparison plot with actual values, following remarks can be emphasized:

1. As a turbulence model, Spalart-Allmaras turbulence model and full factorial design and response surface prediction technique as a statistical estimation tool were found as sufficient tools to understand and to estimate basic fuselage drag characteristics for a low-fidelity study within conceptual design considerations. The effects of upsweep angle, cabin conic parameter and non-dimensionialized versions of cabin length, nose length, cabin width and glass corner radius with respect to cabin height on drag value of a basic fuselage can be estimated via response surface methodology ($p < 0.01$) within certain limits.

2. It has been investigated how the drag characteristics change as a result of the variation of 6 parameters determined for study when the other parameters are held constant. Accordingly, it has been shown that, within the specified limits, the FPDA value increases slightly as the non-dimensionalized cabin length and cabin conic parameter values increase, the FPDA value increases significantly as the non-dimensionalized cabin width and beta values increase, the FPDA values decrease monotonically as the non-dimensionalized glass corner radius value increases, and the change in the non-dimensionalized nose length value does not cause a significant change in the FPDA values.

7.1. Limitations and Future Work

Given plot and obtained equation are valid only in given limits presented in Table 1. In order to get a formula which may have a wider explanation about basic fuselage, a future study can be conducted with more para meters and wider ranges. Generation of the CAD model is an important stage in such a study due to its potential effects on the drag calculations since some deviations and perturbations on the geometry may evoke flow regimes out-of-interest.

Building upon the foundation established through the RSM, this study will extend its scope to encompass a comprehensive comparison with a diverse array of advanced statistical techniques. These methods include Kriging, Gradient Enhanced Neural Networks (GENN), Quadratic Programming (QP), Artificial Neural Networks (ANN), etc. The Python Surrogate Modelling Toolbox (SMT) (Ref. 16), known for its ability to develop accurate surrogate models, is used to streamline the analysis. By synergizing the capabilities of SMT and Scikit-learn (Ref. 17) tools, the research effort aims to speed up the evaluation process, optimize the selection of design factors and ultimately facilitate the identification of optimal design configurations. The objective of this comparison is to evaluate the predictive capabilities, robustness, and computational efficiency of each approach in estimating fuselage drag, similar to the methodology undertaken in (Ref. 18). By utilizing machine learning, the research effort aims to expedite the assessment process, enhance accuracy, and potentially uncover intricate relationships within the dataset that may remain hidden through traditional methodologies.

Author contact:

Fatih Yilmaz fatih.yilmaz4@tai.com.tr

8. REFERENCES

1. *Systems and Software Engineering - System Life Cycle Processes*. ISO 15288:2015, ISO, 2015.

2. *Incose System Engineering Handbook a Guide for System Life Cycle Processes and Activities*, John Wiley & Sons, 2015, Chapter 3.

3. Forsberg, K., Mooz, H., and Cotterman, H., *Visualizing Project Management: Models and Frameworks for Mastering Complex Systems,* John Wiley & Sons, Hoboken, NJ, 2005, Chapter 7.

4. Stepniewski, W. Z., “Civilian Vertical-Lift Systems and Aircraft,” Aeronautica ’73 US/USSR Symposium and Display, Moscow, Russia, July 1973.

5. Keys, C. N., and Wiesner, R., “Guidelines for Reducing Helicopter Parasite Drag,” *Journal of the American Helicopter Society,* Vol. 20, Jan. 1975. DOI: 10.4050/JAHS.20.31

6. Myers, R. H., Montgomery, D. C., and Anderson-Cook, C. M., *Response Surface Methodology*, John Wiley & Sons, Hoboken, NJ, 2016, Chapter 1.

7. Dassault Systemés, CATIA V5 R2012 (R22), Vélizy-Villacoublay, 2012.

8. Siemens Industries Digital Software, Simcenter Star-CCM+ 2021.3 (16.06.008-R8), Plano, TX, 2021.

9. Mineck, R., and Gorton, S. A., “Steady and Periodic Pressure Measurements on a Generic Helicopter Fuselage Model in the Presence of a Rotor,” NASA TM 2000-210286, 2000.

10. Acikgoz, M. B., and Aslan, A. R., “Dynamic Mesh Analyses of Helicopter Rotor-Fuselage Flow Interaction in Forward Flight,” *Journal of Aerospace Engineering*, Vol. 29, June 2016. DOI: 10.1061/(ASCE)AS.1943-5525.0000641

11. Spalart, P., and Allmaras, S., “A One-Equation Turbulence Model for Aerodynamic Flows,” AIAA 30th Aerospace Sciences Meeting and Exhibit, Seattle, WA, January 1992.

12. Myers, R. H., Montgomery, D. C., and Anderson-Cook, C. M., *Response Surface Methodology: Process and Product Optimization Using Designed Experiments*, Wiley Series in Probability and Statistics, 2016.

13. SAS Institute Inc., "JMP," Version 15.1, Cary, NC: SAS Institute Inc., 2019.

14. Maran, J. P., Manikandan, S., Nivetha, C. V., and Dinesh, R., “Ultrasound assisted extraction of bioactive compounds from Nephelium lappaceum L. Fruit peel using central composite face centered response surface design,” *Arabian Journal of Chemistry,* vol. 10, 2017, pp. 1145-1157.

15. “Overview of the Prediction Profiler” JMP Statistical Discovery LLC, Apr. 2023, https://www.jmp.com/support/help/en/17.1/index.shtml#page/jmp/overview-of-the-prediction-profiler.shtml.

16. Bouhlel, M. A., Hwang, J. T., Bartoli, N., Lafage, R., Morlier, J., and Martins, J. R. R. A, “A Python surrogate modelling framework with derivatives,” *Advances in Engineering Software*, 2019. DOI: 10.1016/j.advengsoft.2019.03.005.

17. Pedregosa, F., Varoquaux, G., Gramfort, A., Michel, V., Thirion, B., Grisel, O., Blondel, M., Prettenhofer, P., Weiss, R., Dubourg, V., Vanderplas, J., Passos, A., Cournapeau, D., Brucher, M., Perrot, M., and Duchesnay, E., “Scikit-learn: Machine Learning in Python,” *Journal of Machine Learning Research*, vol 12, pp. 2825-2830, 2011.

18. Zafer, Ö, “Determination of loads on a flexible wing of a fighter jet via surrogate models,” M.S. - Master of Science, Middle East Technical University, 2023.